

## 3. Nuclear astrophysics

Nuclear reactions in stars and stellar explosions generate energy and are responsible for the ongoing synthesis of the elements. They are, therefore, at the heart of many astrophysical phenomena, such as stars, novae, supernovae, and X-ray bursts. Nuclear physics determines the signatures of isotopic and elemental abundances found in the spectra of these objects, in characteristic  $\gamma$  radiation from nuclear decay, or in the composition of meteorites and presolar grains. The field of nuclear astrophysics ties together nuclear and particle physics on the microscopic scale with the physics of stars, galaxies, and the cosmos in a broad interdisciplinary approach. While some of the major open questions of the field have been asked for decades, many others are new, mostly posed by advances in astronomical observations. An example is the discovery of r-process abundance patterns in stars through high-resolution spectroscopic observations with ground-based observatories (for example Keck and VLT) as well as the Hubble Space Telescope. More of these stars are being discovered through extensive surveys, such as the Hamburg/ESO R-process Enhanced Star Survey (HERES) or the ongoing Sloan Extension for Galactic Understanding and Exploration (SEGUE). Superbursts, absorption lines, and ms-oscillations are new phenomena discovered in X-ray bursts by the Chandra X-ray observatory, XMM-Newton, the Rossi X-ray Timing Explorer (RXTE), and Beppo-SAX. Many, if not most of the current open questions of the field require understanding of the physics of unstable nuclei. Though pioneering advances have been made, progress has been hampered by limited beam intensities at current rare isotope beam facilities. The ISF will address this problem and contribute a critical piece of science that together with progress in observations and theory will lead to a major advance in our understanding of the cosmos.

The open questions of the field that most urgently require a better understanding of the physics of unstable nuclei can be broadly organized under three major themes: the origin of the heavy elements, stellar explosions, and neutron stars.

### 3.1 The origin of the heavy elements

#### 3.1.1 The rapid neutron capture process

The rapid neutron capture process (r-process) is one of the major nucleosynthesis processes in nature [Cow91,Qia03]. It produces roughly half of the nuclei found in nature beyond the iron region. While many elements have contributions from multiple processes, there are some that are chiefly produced by the r-process, such as xenon, gold, platinum, and uranium. The fact that the site of the r-process and, therefore, its conditions and reaction sequences are still not known with certainty is one of the major open questions in science. The question of the origin of the heavy elements has been identified in the National Academies report “Connecting Quarks with the Cosmos” as one of the 11 science questions for the twenty-first century at the interface of particle- and astrophysics [BPA03].

##### 3.1.1.1 r-process models

A number of theoretical models have been proposed as sites for the r-process. These include the neutrino-driven wind off a forming neutron star in core-collapse supernovae [Woo92,Tak94], jets in core-collapse supernovae [Cam01], neutron star mergers [Lat77,Fre99], and outflows from rapidly accreting disks in collapsars

powering  $\gamma$ -ray bursts [Sur05]. All these models have been shown to exhibit a rapid neutron capture process within the respective parameter space. However, they all fall short of producing sufficient amounts of r-process elements in the proportions that would explain abundance observations. Clearly more theoretical work is needed to overcome these issues. In the end, however, experimental constraints are needed to guide theory. This requires astronomical observations and a thorough understanding of the nuclear physics underlying the r-process [Kra93].

## Overview of astrophysical processes to be investigated at the ISF

A variety of nuclear processes are responsible for the origin of the elements and for powering stars and stellar explosions. While some important processes such as the fusion reactions in stars or the slow neutron capture process (s-process) proceed with mostly stable nuclei, there are many processes that involve predominantly unstable nuclei. These processes will be the main focus of nuclear astrophysical research at the ISF.

The figure provides a schematic overview of the range of nuclei participating in each process and also indicates the extensive reach of the facility for rare isotope experiments. Clearly, most of the nuclei participating in all of the astrophysical processes can be studied at the proposed facility. Critical processes for the origin of the elements include the rapid neutron capture process (r-process) that produced about half of the nuclei beyond the iron region and was the sole source of uranium and thorium. The p-process was responsible for producing about thirty-five neutron deficient stable isotopes that cannot be produced by neutron capture reactions.

The rapid proton capture process (rp-process) plays an important part in stellar explosions and can, in principle, occur in a number of scenarios. A mild form of the rp-process that reaches nuclei up to  $A \sim 40$  is thought to occur in nova explosions where its products can be observed in the ejecta. A full rp-process, the path displayed in the figure below, is the main energy

source of X-ray bursts. Recently it has been found that an rp-process can also occur in core-collapse supernovae, where it is accelerated by neutron-induced reactions. In this scenario neutrons are generated by neutrino interactions with protons. This vp-process might even proceed beyond the indicated mass range, and might contribute to galactic nucleosynthesis in a significant way.

X-ray bursts that are powered by the rp-process are thought to occur on the surface of neutron stars. Most of the ashes are not ejected by the explosion but are incorporated into the neutron star crust. The ashes then undergo a series of nuclear reactions, mostly electron captures and density-induced fusion reactions. These neutron star crust processes drive the composition, step by step, to the neutron dripline and are an important source of crustal heating.

Electron capture reactions also play an important role in supernova explosions. The figure indicates the region of nuclei that are important in core-collapse supernovae, where electron capture rates affect the dynamics of the collapse. Electron capture reactions on a small subset of stable and unstable nuclei near iron and nickel are also important for Type Ia supernovae, where the electron capture rates affect nucleosynthesis and, possibly, the explosive burning.

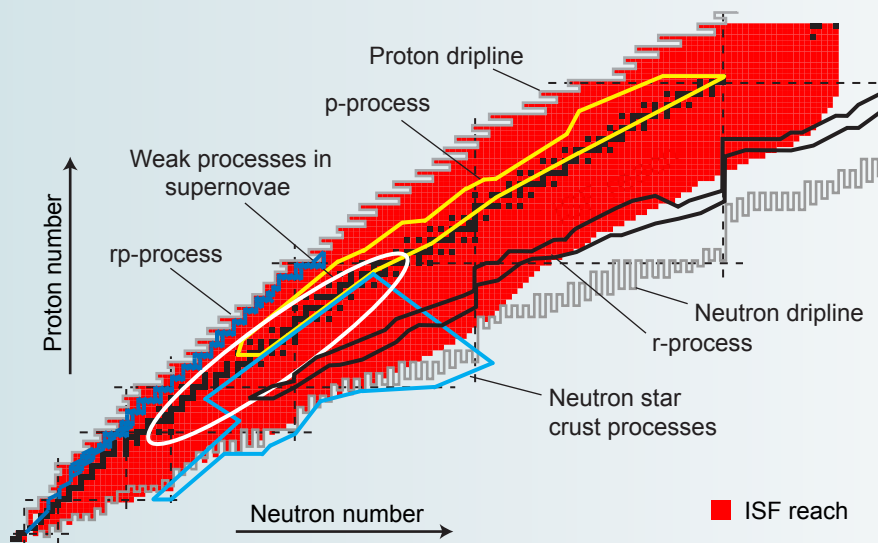


Chart of nuclei with a schematic overview of the major nuclear processes operating in the universe that involve predominantly unstable nuclei. Not shown, for example, are the stellar burning paths or the s-process, which are equally important but involve predominantly stable nuclei. The red area indicates the range of isotopes that will be available at the ISF.

### 3.1.1.2 Precision observations of r-process abundances

There has been tremendous progress on the observational side. Advances in our understanding of the s-process (mainly from measurements of neutron capture cross sections [Kae99] and s-process modeling) make it possible to extract the r-process contribution from the observed solar system abundances with increasing precision. At the same time, the discovery of detailed r-process abundance patterns in some rare, extremely metal-poor halo stars has tremendously broadened the available observational information on the r-process (see [Sne03] as an example and [Tru02] for a review). The material that these stars illuminate in their photosphere has been polluted by a single, or at most very few, r-process events. Provided the nuclear physics is at hand, this opens the door for comparing r-process model predictions with individual r-process events. In addition, the observations open a window to study the history of the operation of the r-process in our Galaxy. First results indicate that there might be two r-processes contributing to the solar system abundances [Pfe01, Tra04]. This is in line with evidence from meteoritic data on the decay products of radioactive r-process isotopes [Qia98]. In the coming years, ongoing surveys such as SEGUE will lead to the discovery of many more such r-process enhanced metal poor stars, which will allow one to study the behavior of the astrophysical events that created the r-process nuclei in detail.

### 3.1.1.3 Nuclear physics of the r-process

Similar progress is needed in our understanding of the nuclear physics of the r-process. Figure 3.1 demonstrates the sensitivity of r-process model calculations

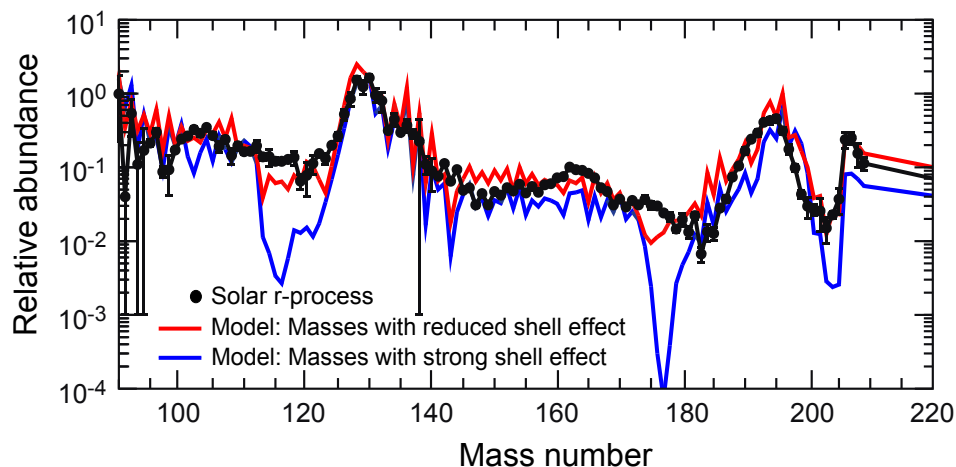
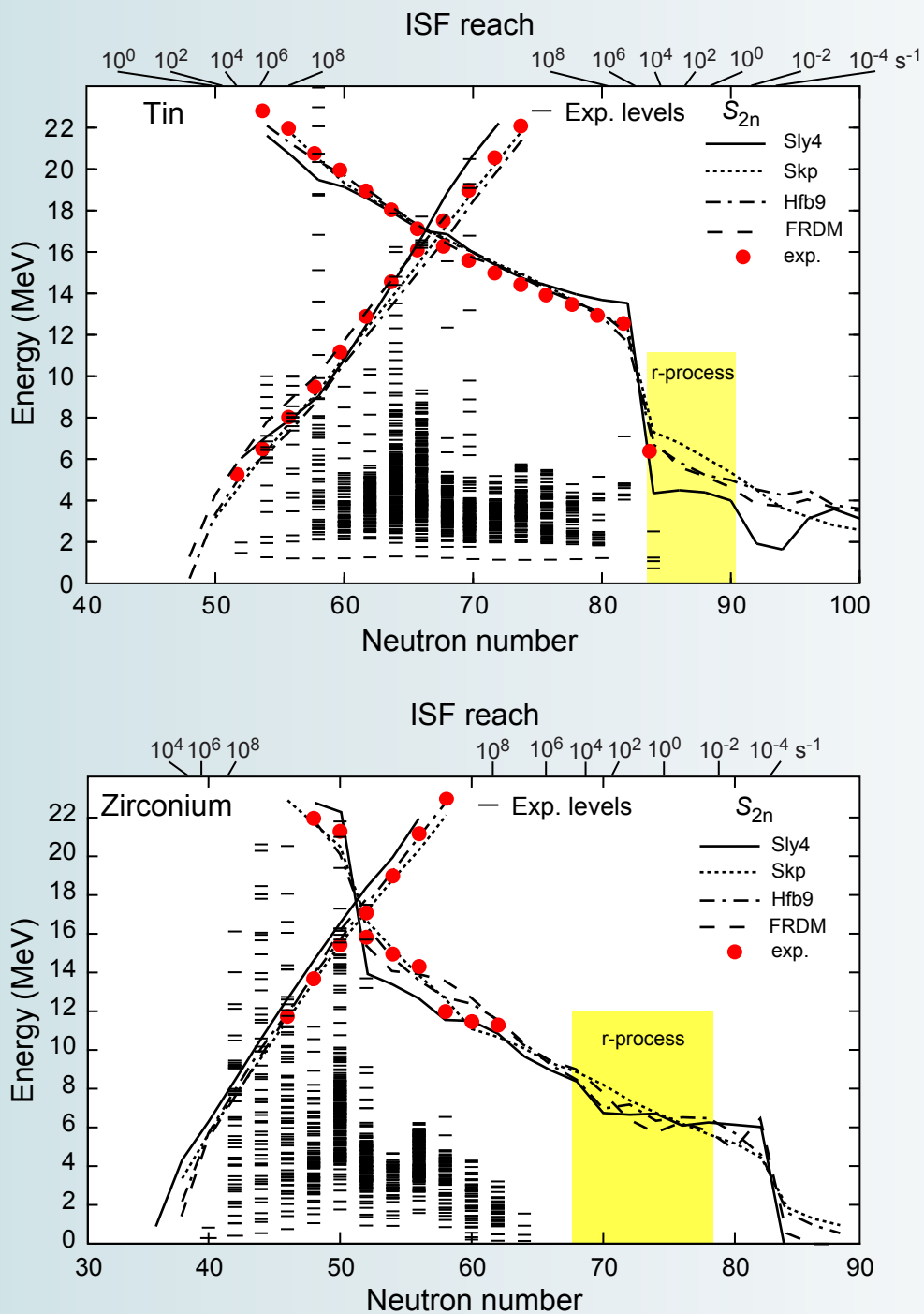


**Figure 3.1:** Influence of shell structure on r-process calculations. The black dots represent the contribution of the r-process to the observed isotopic abundances of the chemical elements in the solar system as a function of the mass number (“solar r-process”). This distribution is obtained by subtracting calculated contributions from the s-process and other, less important, processes from the observed solar abundance distribution. The abundances are given in usual units relative to one million silicon nuclei. In addition, we show the calculated abundances produced in two r-process models that only differ in the theoretical model used to predict the nuclear masses. One mass model shows pronounced shell closures, while the other has a reduced shell closure effect that might occur for very neutron-rich nuclei. All the relevant masses for the model discrepancies below  $A \sim 130$  are either within reach at the ISF or can be extrapolated reliably. This will remove the nuclear physics uncertainty in r-process models so that the remaining differences to observations can be interpreted in terms of the nature of the r-process and its astrophysical site. Adapted from [Che95, Kra06].

## Theoretical reach toward the dripline



The figures illustrate our present knowledge of even- $N$  tin (top) and zirconium (bottom) isotopes together with the region of interest for the  $r$ -process. Observed energy levels for even-even nuclei are shown with the first excited states being  $2^+$ . The relatively high  $2^+$  energies at  $N = 50$  and  $N = 56$  for zirconium and  $N = 82$  for tin are indications of the shell gaps at these magic numbers. Measured two-nucleon separation energies are indicated as red circles with two-proton separation energies extending up from the proton dripline on the left and the two-neutron separation energies going down to the neutron dripline on the right. The two-nucleon separation energies predicted by three different Skyrme interaction models [Dob04,Gor06] and the Finite-Range Droplet Model (FRDM) [Mol95] are shown by the lines. The source of the deviation for Sly4 from experiment near the magic numbers is partly understood and might be corrected by including ground-state correlations. For the regions of interest in the  $r$ -process, the predictions show divergences related to uncertainties in shape transitions and pairing energies that can be confronted by comparison to new experimental data from the ISF.

on the underlying nuclear physics assumptions. The critical nuclear physics are masses and decay properties (half-lives and branchings for  $\beta$ -delayed neutron emission), which determine path, timescale, and the abundance pattern produced by the r-process. Neutron capture rates play a role during freezeout. Depending on the scenario, fission rates and fragment distributions as well as neutrino interaction cross sections might be relevant as well. Knowledge of nuclear physics is specifically needed to answer the following questions:

- What are the abundances produced in the r-process for a given astrophysical model?
- What are the constraints on the conditions during the r-process as inferred from the observed abundances in the solar system and in stars?
- What are the individual contributions of the multiple r-processes that together with the s-process might produce the elements below barium?

As Figure 3.2 shows, only very few of the critical  $\beta$ -decay half-lives in the r-process are known today, severely limiting the ability of r-process models to predict abundance signatures. In recent years it has become possible to reach the r-process path with experiments for a wider range of elements between the  $N = 50$  and  $N = 82$  shell closures, mainly by making use of fragmentation beams at the NSCL [Hos05,Mon06b]. At the same time, ISOL facilities have continued to provide important data on critical isotopes in regions particularly suitable for that technique, for example, for the neutron-rich cadmium or tin isotopes [Dil03,She02,Kra00]. These few experiments have already put first experimental constraints on r-process models related to the processing time to form the  $A \sim 80$  and  $A \sim 130$  abundance peaks. Mass measurements require higher beam intensities than half-life measurements, reducing the experimental reach to isotopes with three to five fewer neutrons. Consequently mass measurements have reached the path of the r-process only in a few cases near shell closures [Sik05a,Dil03].

Within the next few years we can expect that existing facilities, such as the NSCL CCF, will continue to extend the border of known half-lives about halfway into the r-process path in the  $N = 50$ – $82$  range. While this will be an important step forward, many of the most neutron-rich nuclei in the critical region just below the  $A = 130$  abundance peak (see Figure 3.1) as well as the entire r process beyond  $N \sim 90$  will remain out of reach (see Figure 3.2). In addition, in any mass region of the r-process, most of the nuclear masses will remain inaccessible.

As shown in Figure 3.2, the picture would dramatically change with the fast beam capabilities of the ISF. At the ISF, all r-process nuclei up to  $A \sim 140$  would be within reach for half-life measurements and most of them for mass measurements. For example, at the ISF all the masses of nuclei with  $N \leq 82$  could be measured down to technetium (see also Section 2.3.1), providing data for neutron separation energies directly in the exotic  $N \leq 82$ ,  $Z \leq 44$  region, where differences in the trends of mass predictions due to nuclear structure effects lead to the notorious discrepancies in r-process model predictions for abundances below the  $A = 130$  peak (see Figure 3.1). This would unambiguously settle the issue of the possible quenching of the  $N = 82$  shell gap far from stability and its influence on the r-process (see also Section 2.3).

With the fast beam capability of the ISF it will be possible to measure many new half-lives in a single experiment using a mixed fragment beam. The different

## Observations of r-process elements in stars

Observations of elemental abundances in very metal-poor stars are revolutionizing the field of nuclear astrophysics. Metal-poor stars are found among lower-mass stars in the halo of our Galaxy, where they formed within a few hundred million years after the Big Bang. At that time, the enrichment of iron in the Galaxy through supernova activity had not progressed very far. Thus, these stars have preserved information on the chemical composition at that specific location in the Galaxy at the time of their formation. The metal-poor halo stars, therefore, offer a way to look back in time and observe the products of nucleosynthesis in the first epochs of the chemical evolution of our Galaxy.

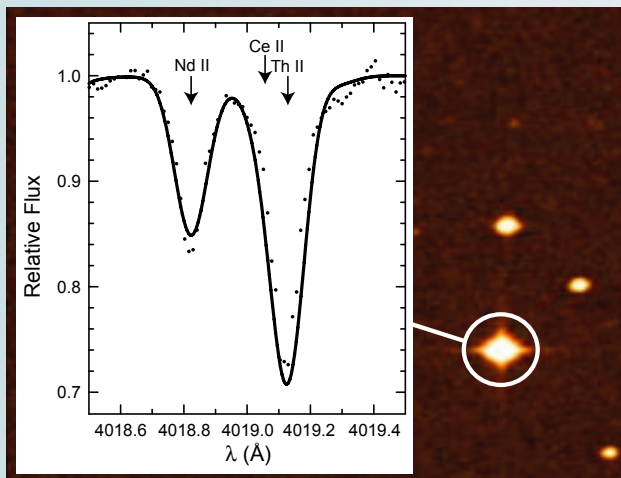


Figure A: A small portion of a high-resolution spectroscopic observation of the very metal-poor halo star CS 31082-001, obtained with the European 8 m VLT telescope, showing one of the eleven detectable absorption lines of the r-process element thorium (Th II) in this star. Comparisons of r-process model predictions based on experimental nuclear data with the observed element abundances constrain the r-process model conditions and, in the case where both thorium and uranium are detected, the age of these elements. Because these stars are extremely old, the latter also provides a lower limit for the age of the universe. Insert adapted from [Cay01,Bee06]. Image of star: This data is copyrighted by the Space Telescope Science Institute (STScI Digitized Sky Survey, © 1993, 1994, AURA, Inc. all rights reserved).

These very metal-poor stars that exhibit factors of 10–100 times more r-process elements than found in the Sun are especially interesting. They provide a glimpse of the elemental composition that may have been produced by a single r-process event in the early Galaxy. Figure A shows an example of the clear spectral signature of thorium, an element that can only be produced in the r-process, from one of these stars. Another prime example is the star labeled CS 22892-052, from which 57 elemental abundances have been determined to date. Figure B compares the observed abundance levels with the r-process contribution to elements in the Sun, which is thought to be a superposition of many r-process events. Although there are discrepancies for lighter elements, the abundances match for very heavy elements beyond barium. This provides important clues about the nature of the r-process.

The discrepancies among the distributions of lighter r-process elements have been interpreted as a hint that a second r-process might produce the missing abundances. However, matching the observations with r-process model calculations and attempts to use such calculations to disentangle the contributions of different r-processes have been hampered by the lack of nuclear data for the very neutron-rich nuclei.

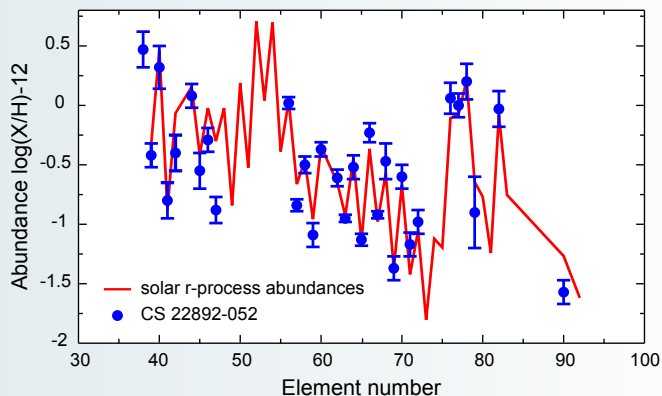
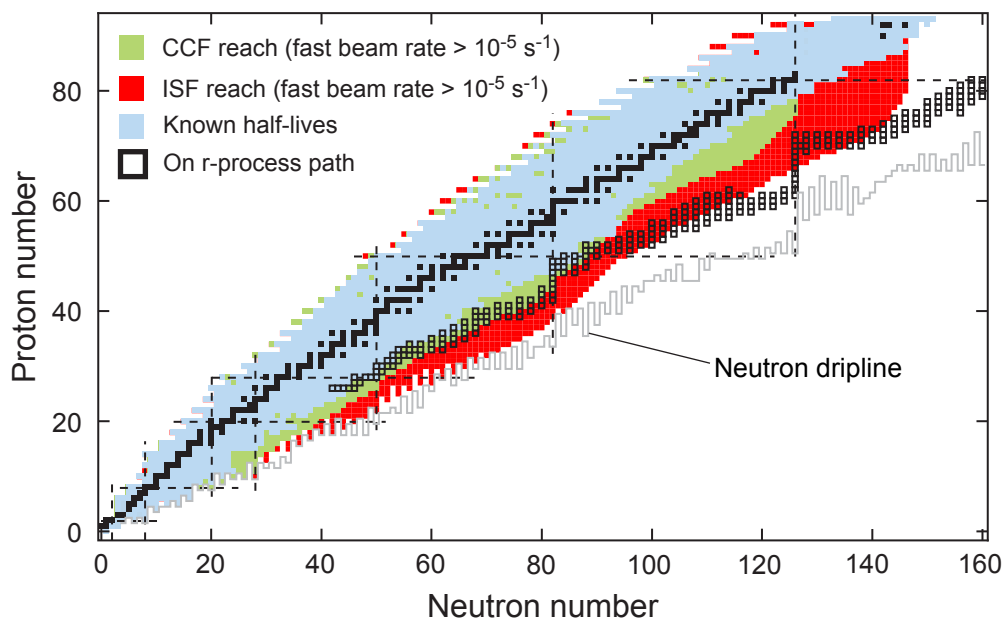


Figure B: The observed elemental abundances in the very-metal poor r-process enriched halo star CS 22892-052 (blue data points). For comparison, the contribution of the r-process to the solar system elemental abundance distribution is also shown (red curve). Clearly the surface composition of the star for heavy elements with  $Z > 37$  is entirely determined by the r-process. Adapted from [Sne03,Cow06].

The few observations of thorium and uranium in metal-poor r-process-element enriched stars offer the possibility to determine the age of the r-process event that contributed to that star. Such an age determination requires a reliable r-process model that can predict the initial r-process abundance of thorium and uranium. Comparison of the predictions with the observed abundance then allows one to use the known nuclear decay rates to determine the age. Because these stars are so old, this method can provide an independent constraint on the age of the Galaxy and the universe. However, the reliable prediction of uranium and thorium production in the r-process is severely limited by a lack of nuclear data, especially for the r-process waiting point nuclei around  $N = 126$ , the last point of normalization of the r-process before entering the actinide region. This problem will be addressed by experiments at the ISF.

To date, only a handful of r-process element-enhanced, very metal-poor stars have been found. A larger sample is needed to explain the enrichment of the Galaxy with r-process elements over time and to explain variations and similarities among r-process events. Unfortunately, only about one in about 1.2 million halo stars is both r-process enriched and very metal-poor. Nevertheless, with ongoing powerful surveys such as SEGUE, there is the hopeful intention to identify and analyze hundreds of such stars in the near future. Large-scale surveys based on low- and medium-resolution spectroscopy locate the most promising candidates. Then, 8–10 m class telescopes are used to determine accurate element abundances from high-resolution spectra. The ISF will provide the nuclear data needed to fully interpret these observational data and to compare them with r-process models.



**Figure 3.2:** Reach of the ISF into the r-process path. Shown are nuclei with known  $\beta$ -decay half-lives (blue) and nuclei that are within reach for half-life measurements, either at existing facilities (NSCL, green), or at the ISF (red), assuming fast beams are used. Important nuclei in a typical r-process [Sch02] are indicated by thick open squares.

species can be easily disentangled using event-by-event particle identification, a well-developed technique that has been frequently used in the past [Fae02,Hos05, Mon06b,Sor93]. It will therefore be possible to measure all the half-lives marked in Figure 3.2 in a series of experiments over the lifetime of the ISF. This is important for r-process studies, because the reliable calculation of a wide range of abundances forming the characteristic abundance pattern is needed to extract all the information contained in observations.

In particular, the half-life and mass data from the ISF, together with mass extrapolations by a few isotopes, would allow one to reliably calculate the entire r-process up to  $A \sim 140$ . This is a critical mass range, where signatures from freeze-out timescales [Fre99], neutrino post-processing [Qia97], and possibly fission of nuclei at the endpoint of the r-process would be particularly prominent. Comparison with precision observations will then allow one to detect these signatures and to test r-process models. In addition, multiple r-processes might contribute to the observed abundances in this mass range. With the data from the ISF, contributions from individual processes could finally be disentangled reliably in a way similar to that in which the nuclear physics in the s-process is used today to disentangle s- and r-process contributions to the solar abundances.

As Figure 3.2 also shows, with the ISF, a range of r-process nuclei at the  $N = 126$  shell closure also come into reach. This region is associated with the  $A = 196$  abundance peak and represents the last bottle-neck for the r-process before proceeding into the lead and actinide region. It is therefore a critical normalization point for r-process models, especially for the prediction of the endpoint of the r-process and the production of uranium and thorium, which have been used as cosmic chronometers in the past [Cow91,Kra04]. All of the  $N = 126$  r-process waiting points have been out of reach at existing facilities to date. While the ISF cannot reach all

---

$N = 126$  waiting points for half-life measurements, the ones that are within reach are closer to stability and are, therefore, expected to be the major contributors to the overall timescale for the r-process to pass through that region. In addition, the greatly improved understanding of nuclear structure, not only in the  $N = 126$  region but also for lighter nuclei will allow much more reliable calculations of the  $\beta$ -decay properties and masses that will remain out of reach experimentally.

Neutron capture rates can play a role in some r-process models during freeze-out when the equilibrium between neutron capture and  $(\gamma, n)$  photodisintegration breaks down. During this phase, late-time neutron captures can modify the final abundance distribution somewhat [Fre99]. While neutron capture rates on short-lived unstable nuclei cannot be measured directly, experiments can provide critical information to estimate the reaction rates. Inverse kinematics  $(d, p)$  reactions at energies from 4–10 MeV/nucleon have been used in the past to obtain information on spectroscopic factors and to determine neutron capture rates for astrophysical purposes [Gau06, Ciz05]. Intensities of reaccelerated fragmentation beams at the ISF will be sufficient ( $> 10^4 \text{ s}^{-1}$ ) to perform such measurements on a wide range of neutron-rich nuclei that over much of the  $Z = 28$ –52 range comes within one to two isotopes of the main r-process path and, in a few cases, reaches it.

With fast beams at the ISF, one can probe dipole strength distributions via Coulomb excitation techniques over a similar range (see Section 2.3.2.1). In particular, the possible shift of  $E1$  strength towards lower excitation energies for neutron-rich nuclei can influence the prediction of neutron capture rates for r-process calculations and needs to be understood [Gor98] (see Section 2.5.4.3). Together, these experiments will allow one to systematically test model predictions of neutron capture rates along isotopic chains up to the path of the r-process.

### 3.1.2 The p-process

Thirty-five neutron-deficient stable isotopes found in nature, ranging from  $^{74}\text{Se}$  to  $^{196}\text{Hg}$ , cannot be produced via neutron-capture processes. These relatively rare isotopes originate in the p-process, thought of as a process of  $(\gamma, n)$ ,  $(\gamma, p)$ , and  $(\gamma, \alpha)$  reactions acting on a seed of s-process nuclei, most likely in explosive O-Ne burning in core-collapse supernovae [Arn03]. Current p-process models can reproduce most of the observed abundances to within a factor of four only. A particular long-standing problem in nuclear astrophysics is the underproduction of the proton-rich isotopes of molybdenum and ruthenium by about an order of magnitude.

The critical nuclear physics in the p-process are the rates of  $(\gamma, p)$ ,  $(\gamma, n)$ ,  $(\gamma, \alpha)$ , and  $(n, p)$  reactions. Reaction rates involving  $\alpha$  particles are especially difficult to predict reliably, due to uncertainties in the  $\alpha$  potentials used in statistical model calculations. Many of the important reaction rates, in particularly the  $(\gamma, \alpha)$  chains that drive matter from heavy nuclei towards lighter nuclei, involve unstable nuclei [Rap06]. Nuclear data for the p-process are needed to:

- analyze observed p-process abundances in terms of other model deficiencies, such as the assumption of the seed abundance distribution or the temperature and density evolution in a particular model;
- test various alternative p-process models, such as the pre-explosive p-process in massive stars, accretion disks around black holes, type Ia

supernovae, or the collapse of a white dwarf induced by accretion of helium from a companion star by comparing abundance predictions with observations.

At existing facilities, the limited beam intensities leave Coulomb Dissociation [Bau96] as the only choice for the measurement of p-process reaction rates on unstable targets and with unstable final nuclei. Such measurements can in principle be performed with beam intensities of the order of  $10^4 \text{ s}^{-1}$ . It remains to be demonstrated that this method is suitable for heavy unstable nuclei near stability, where reaction rates are typically dominated by many resonances. Experiments are currently underway to investigate this issue [Son06]. If successful, existing facilities could apply this technique over the coming years to a number of p-process reaction rates. Fast beam intensities at the ISF are sufficient to easily measure all critical p-process reaction rates via Coulomb breakup. However, the Coulomb breakup technique relies on theoretical assumptions about the relevant multipolarities and  $\gamma$ -ray cascades when applied to resonant rates with well-bound nuclei and high level-densities.

At the ISF, intense ( $10^{8-9} \text{ s}^{-1}$ ) reaccelerated beams at astrophysical energies also become available for most of the p-process path. This will open the possibility for direct measurements of  $(p,\gamma)$  and  $(\alpha,\gamma)$  reaction rates in inverse kinematics on proton or helium targets, respectively. The measured rates can then be related to the inverse  $(\gamma,p)$  and  $(\gamma,\alpha)$  reaction rates via the detailed balance principle. In this case, a theoretical correction is required that accounts for the stellar enhancement factor due to the thermal population of the target nucleus in a stellar environment. The direct measurement of the particle capture rates is complementary to the measurement of the photodisintegration rates via Coulomb Breakup. Combining both methods will provide the necessary cross-checks to address model dependencies and theoretical uncertainties. At the ISF, all the reaction rates identified in recent p-process studies as important [Rap06], for example  $^{126}\text{Ba}(\gamma,p)$ ,  $^{110}\text{Sn}(\gamma,p)$ ,  $^{104}\text{Cd}(\gamma,p)$ ,  $^{100}\text{Pd}(\gamma,p)$ , and  $^{122}\text{Xe}(\gamma,\alpha)$  would be accessible for this approach.

Because of the problems of using “standard” p-process scenarios to predict all the observed abundances of nuclei in the solar system that originate in the p-process, a range of alternative sites has been explored in the past. This includes the rp-process in X-ray bursts that had been proposed as an alternative site for the nucleosynthesis of lighter p-process nuclei in the molybdenum-ruthenium region (see Section 3.2.1). More recently, it has been shown [Pru05,Fro05] that during the early stages, the neutrino-driven wind off a forming neutron star in a core-collapse supernova represents a proton-rich environment. In these proton-rich outflows, nucleosynthesis through an rp-process can occur. This is similar to the r-process thought to occur in the same scenario at later stages when the outflow becomes neutron rich. So the neutrino-driven wind can eject, at early times, rp-process ashes and, at late times, r-process ashes. Such an rp-process can possibly contribute to the nucleosynthesis of some proton-rich isotopes such as  $^{45}\text{Sc}$ ,  $^{49}\text{Ti}$ , and  $^{64}\text{Zn}$ . In addition it was shown [Fro05] that neutrino interactions generating neutrons and the associated neutron-induced reactions can bridge the major waiting points, for example  $^{64}\text{Ge}$ , and result in reaction flows that might reach the lighter p-nuclei, including neutron-deficient molybdenum and ruthenium isotopes. This vp-process might even explain the strontium, yttrium, and zirconium abundances observed in very metal-poor stars that have been shown to not originate from the traditional s- or r-processes [Tra04].

---

Accurate nuclear physics is needed to calculate the abundance signatures of this scenario and to determine whether this indeed provides the solution to the long-standing puzzles of the origin of neutron-deficient molybdenum and ruthenium isotopes in the solar system and the observations of strontium, yttrium, and zirconium in stars [Tra04]. We are just beginning to delineate the nuclear physics needed to predict nucleosynthesis in this new scenario. Current models indicate a reaction flow resembling an rp-process, at least up to the tin region. In this case, the capabilities outlined in connection with the rp-process in X-ray bursts (see section 3.2.1) will also address an important part of the nuclear physics needed in proton-rich neutrino-driven winds.

## 3.2 How do stars explode?

### 3.2.1 X-ray bursts and superbursts

X-ray bursts are among the most interesting explosive astrophysical phenomena in our Galaxy [Str03,Sch06a]. With dozens of sources bursting regularly or irregularly, with recurrence times of hours to days, they are the most frequent thermonuclear explosions known. The brightness, frequency, and the fact that the same source can be repeatedly observed with different telescopes makes them a unique testing ground for explosive nuclear burning at extreme temperatures and densities. X-ray bursts occur on the surface of neutron stars accreting matter from a close companion star [Str03] (see Figure 3.3). X-ray bursts and the associated phenomena provide, therefore, a unique window into the physics of neutron stars. Not only do they probe neutron stars in different ways, but unlike isolated neutron stars that are constrained in properties by the formation mechanism, the mass accretion process changes the spin, mass, and thermal structure of the neutron star, considerably broadening the parameter space for neutron star studies.

X-ray bursts occur in a layer of often hydrogen- and helium-rich material that is accreted onto the surface of the neutron star. After a few hours of accretion, the material ignites and hydrogen and helium burn into heavier elements in a thermonuclear explosion that typically lasts for 10–100 s. The released nuclear energy powers an observable X-ray burst with an energy of  $10^{39}$ – $10^{40}$  ergs (about the energy that the Sun emits in a month).

There are many open questions concerning the variety of burst timescales, light curve shapes or recurrence time behavior. The role of multidimensional effects such as ignition points, the spreading of the burning front across the star, or rotation is also not understood. In addition, a range of discoveries and new observational data by X-ray observatories, such as Beppo-SAX, RXTE, Chandra, and XMM-Newton, have revolutionized this field and dramatically broadened the range of known nuclear physics-driven phenomena. Examples include the discovery of millisecond oscillations during X-ray bursts [Str04], the detection of absorption lines that provide information on the surface composition and the gravitational redshift [Cot02], and the discovery of superbursts – extremely rare but about a factor of 1000 times more powerful X-ray bursts [Int04].

To interpret these phenomena and to address the many open questions, the astrophysics and the underlying nuclear physics need to be understood. Data from observations and from experimental nuclear physics are therefore needed. This is illustrated in Figure 3.4. The high quality observation of an X-ray burst light curve

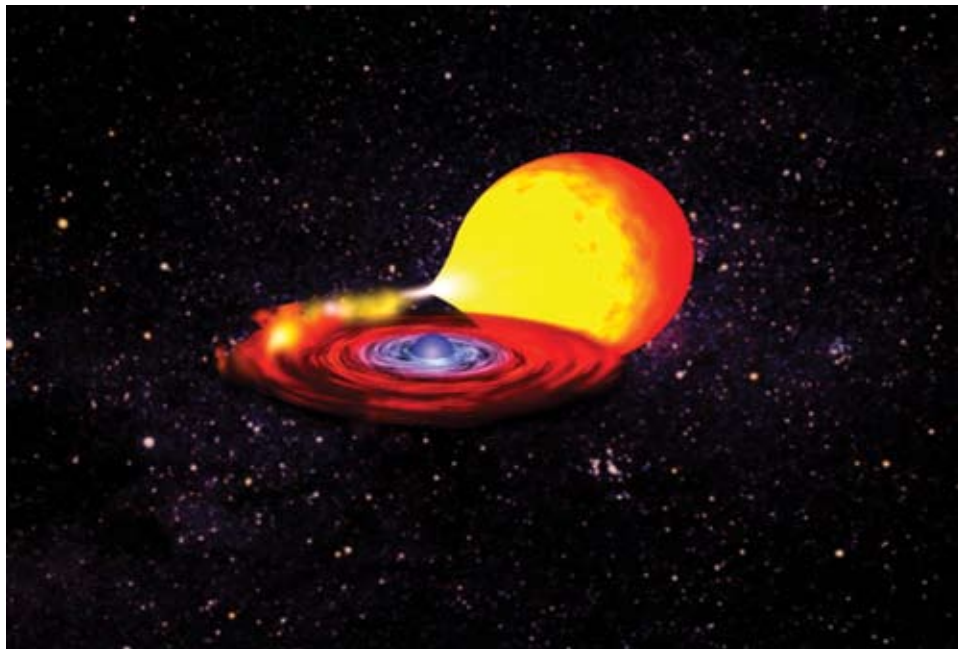


**Figure 3.3:** Artists view of an accreting neutron star in an X-ray binary system. The companion star (orange) has expanded and matter overflows through an accretion disc onto the surface of the neutron star (purple). Image used by permission of NASA.

and its changes over the years due to changes in the accretion rate provide the possibility of precision tests of X-ray burst models [Gal04]. However, the nuclear physics is still far from being accurate enough to perform such precise tests, as shown in the right panel of Figure 3.4 [Bro02a,Woo04].

Recent progress in theory has led to predictions of additional signatures of nuclear burning during X-ray bursts. It has been shown that ejection of some burned material during winds in particularly luminous radius expansion bursts could lead to observable signatures in the X-ray spectra [Wei06]. In addition, it has been found that the detailed composition of the burst ashes can greatly influence heating in the crust, affecting several observables, for example superbursts (see Section 3.3.1). Experimental data on the nuclear physics of X-ray bursts are therefore needed to:

- Understand the wide variety of observed X-ray burst light curves and interpret them to test X-ray burst models and to constrain system properties, such as the accreted composition. For example, the amount of hydrogen in the accreted matter is critical for determining distances [Gal06b] and to constrain the neutron star compactness and the equation of state for dense nuclear matter [Oze06]. The shape of the burst light curve can provide unique diagnostics of the amount of accreted hydrogen, provided one has a reliable burst model. However, it is also sensitive to the nuclear physics of the rp-process (see Figure 3.4) [Sch01], which needs to be well understood.
- Reliably calculate the composition of the burst ashes, which is a prerequisite for understanding all processes that occur deeper in the crust, such as superbursts or crustal heating (see Section 3.3.1).

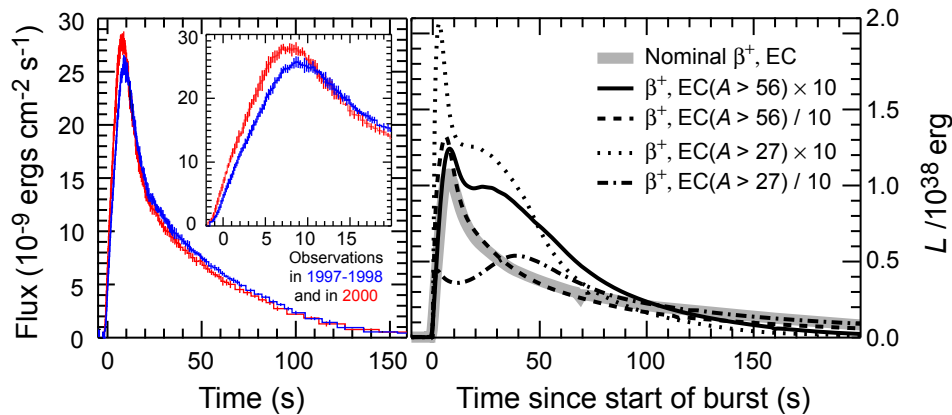


**Figure 3.4:** The left panel shows precision observations of X-ray burst light curves from GS 1826-24 by the RXTE observatory. The observations reveal systematic light curve changes from observations in the years 1997-1998 (blue) to observations in 2000 (red) that are likely related to changes in the accretion rate. Such measurements provide an excellent testing ground for X-ray burst models. The panel on the right shows predictions of X-ray burst light curves from state-of-the-art one-dimensional model calculations. The various curves are obtained for different assumptions on the nuclear physics of the rp-process. To approximate nuclear physics uncertainties that influence the effective lifetimes of the nuclei in the rp-process,  $\beta^+$  and electron capture rates of two groups of nuclei (with  $A > 56$  and with  $A > 27$ ) have been increased and decreased by a factor of ten. Current precision in nuclear physics is not adequate to fully interpret the observations. Adapted from [Gal04,Gal06a] (left) and [Woo04] (right).

The nuclear processes driving X-ray bursts are the  $\alpha p$ - and rp-processes [Wal81] proceeding along the proton dripline, in some bursts up to tellurium [Sch01,Woo04]. Masses, half-lives, and reaction rates for  $(p,\alpha)$  and  $(\alpha,p)$  reactions on unstable nuclei are important. See [Cha92,Sch98,Wie98,Sch06a] for more general reviews, [Sch06b] for the importance of masses, [Wie99b] on breakout reactions from the CNO cycles, and as an example [Fis06,Coo06] for the importance of a single reaction rate – in this case  $^{15}\text{O}(\alpha,\gamma)$ . The vast majority of half-lives have already been measured, and most of the masses are coming within reach at existing facilities. This has already led to important progress in the understanding of X-ray bursts. For example, mass and lifetime measurements around the key waiting point nuclei  $^{64}\text{Ge}$ ,  $^{68}\text{Se}$ , and  $^{72}\text{Kr}$  have already established that together these nuclei are likely to impose considerable delays in the rp-process (see [Sch06b] for a review). This has led to the interpretation of frequently observed, rather long X-ray bursts ( $\sim 100$  s) as signatures for an extended rp-process and, therefore, the presence of significant amounts of hydrogen at ignition (for example [Sch01]). This constrains the burning regime and the nature of the companion star (hydrogen-rich), and can improve distance estimates as the maximum possible burst luminosity is determined by the composition of the accreted material.

However, charged particle induced reaction rates have been difficult to measure because of the limited intensities of rare isotope beams (see review in [Sch06a] and discussion in Section 3.2.3). Most rates in the rp-process are still based exclusively on theory, and in most of the remaining cases experimental information needs to be complemented with theory. Theoretical predictions of rp-process reaction rates are extremely unreliable. Shell model calculations, which can be used up to  $A \sim 60$ , can predict excitation energies of resonant states. However, reaction rates are so

sensitive to resonance energies that the rather small uncertainties in the shell model predictions of around 100 keV still can translate into reaction rate uncertainties of many orders of magnitude. In addition,  $\alpha$  strengths and the weak proton strength of some important resonances are difficult to calculate accurately. Beyond  $A \sim 60$ , statistical models are used to predict reaction rates, even though level densities near the proton dripline are too small for such an approach to be applicable. It is therefore essential to determine reaction rates experimentally.

Figure 3.5 shows the path of the reaction flow during an X-ray burst [Sch01] together with the intensities for reaccelerated beams at the ISF. A few of the reaction rates might be within reach at existing facilities (see discussion in Section 3.2.3). At the ISF, intensities of low energy reaccelerated beams will be sufficient to perform direct measurements of the vast majority of the relevant reaction rates up to  $A \sim 40$ , and on some rates up to  $A \sim 56$  (see also Section 3.2.3).

In addition, the vast majority of the remaining reaction rates can be investigated by indirect techniques. Examples are Coulomb dissociation or neutron removal reactions with fast beams, which have been well established at existing facilities [Del93,Sch06c,Dav01,Mot04,Cle04]. Transfer reactions performed with lower energy reaccelerated beams, such as  $(d,n)$ ,  $(d,p)$ , or  $({}^3\text{He},d)$  can be used to extract

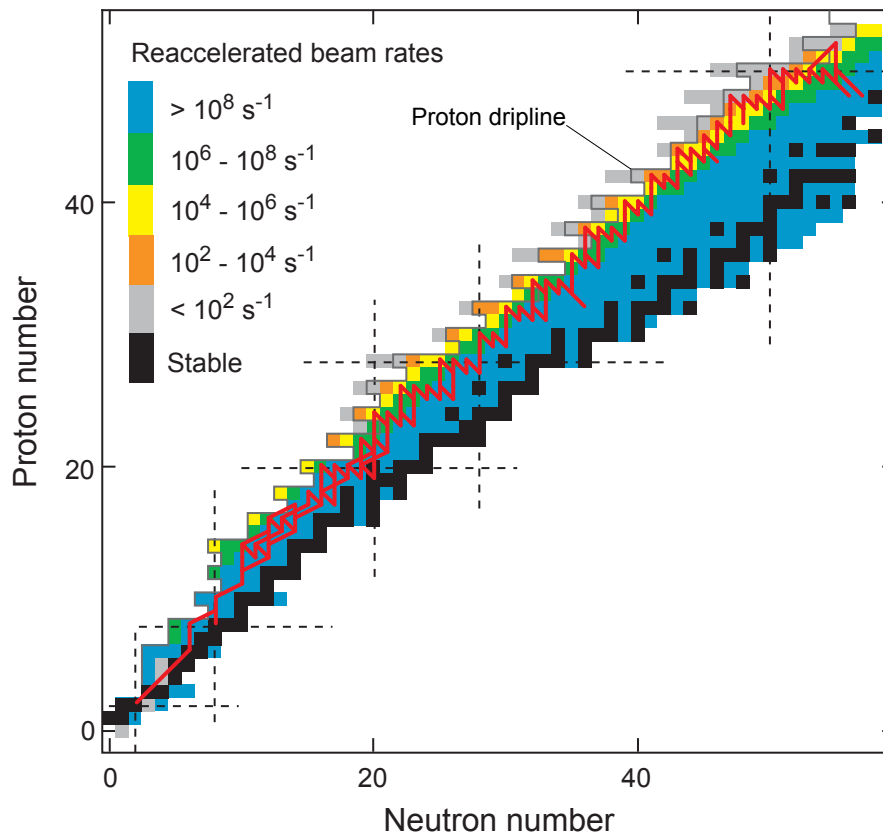


**Figure 3.5:** The time integrated reaction flow (solid red line) during an X-ray burst with particularly large amounts of hydrogen available at ignition [Sch01]. This calculation delineates the maximum extent of the rp-process that ends in a Sn-Sb-Te cycle. The colors indicate the intensities of low energy reaccelerated beams at the ISF. Direct measurements of reaction rates in inverse kinematics require at least  $10^7$ – $10^8$  s<sup>-1</sup>, often much more. Indirect techniques can already be applied with beam intensities in excess of  $10^4$  s<sup>-1</sup>. The dashed lines indicate the classical shell closures.

---

proton spectroscopic factors, ANCs, or neutron spectroscopic factors in mirror nuclei (for example [Reh98,Muk06]). These techniques typically require beam intensities of at least  $10^{4-5} \text{ s}^{-1}$ . A particularly important region that will become accessible to extensive experimental investigations is that around the critical waiting points  $^{64}\text{Ge}$ ,  $^{68}\text{Se}$ , and  $^{72}\text{Kr}$ . These waiting points shape X-ray burst light curves and determine the amount of heavier nuclei produced. They can be strongly affected by proton capture rates [Sch06b] that are largely out of reach at existing facilities. Coulomb breakup measurements with fast beams would be especially important to determine proton capture rates on proton unstable targets with lifetimes below a few hundred nanoseconds, such as  $^{69}\text{Br}$  or  $^{73}\text{Rb}$ .

In addition, all the nuclear masses in the rp-process will be within reach for precision Penning-Trap based measurements at the ISF (see Section 2.3.1). This includes the heaviest relevant neutron-deficient nuclei around and just below  $^{100}\text{Sn}$ , which are also relevant for the vp-process (see Section 3.1.2) and might still be out of reach at existing facilities. By combining, in a coordinated approach, the mass measurements, direct measurements of reaction rates on lighter targets, and a complementary range of indirect techniques applied to heavier targets taking advantage of both fast beams and reaccelerated beams, the vast majority of the nuclear data needed to model X-ray bursts reliably would become available.

### 3.2.2 Supernovae

Supernovae play a critical role in our understanding of the universe. They are the major sources of nucleosynthesis and, possibly, cosmic rays. They create neutron stars and black holes, and their shockwaves are among the main drivers of galactic chemical evolution and mixing. Supernovae are extremely bright and energetic, and are characterized by some of the most extreme conditions encountered anywhere in the universe. There are two major classes of supernovae. Core-collapse supernovae are the result of the collapse of the iron core of a massive star at the end of its evolution. Thermonuclear supernovae are powered by explosive carbon and oxygen burning of a white dwarf that through accretion of matter reaches a mass beyond the limit where electron pressure can balance gravity, the Chandrasekhar mass limit. Thermonuclear supernovae (observationally classified as type Ia) can be used as cosmological standard candles using measurements of their light-curve behavior. They serve therefore as cosmological distance indicators. Together with other observations, this has led to the discovery that the universe is undergoing an accelerating expansion and is dominated by dark energy [Lei01b].

For both types of supernovae, the driving mechanism is not well understood, and in both cases, nuclear physics, such as the equation of state and weak interactions, play an important role.

#### 3.2.2.1 Core-collapse supernovae

We know that the majority of nuclei in the universe, including possibly the heavy elements made in the r-process, originate from core-collapse supernovae. But we do not yet understand the mechanism that transforms the gravitationally powered collapse into an explosion that ejects the outer layers of the star. Weak interactions surely play an important role in this scenario. As regulators of electron density, they help set the dynamics of the collapse and the amount of material the outgoing shock must traverse. The importance of accurate weak interaction rates has been

demonstrated by detailed simulations indicating that important core-collapse characteristics change when new shell model electron capture rates are used in place of earlier values [Heg01,Hix03]. Reliable estimates for electron capture rates are therefore among the important physics ingredients needed to judge the failure or success of a given supernova model.

Late in the precollapse evolution of a massive star, nuclei in the iron-mass range play the major role in capturing electrons. As the collapse proceeds toward nuclear density, nuclear statistical equilibrium shifts to heavy neutron-rich nuclei beyond  $A \sim 60$ , and a broad range of stable and neutron-rich nuclei becomes important. For the later phases of the collapse this became clear recently, when more realistic theoretical electron capture rates were incorporated in supernova models. Before, it had been the prevailing wisdom that weak interactions involving free protons and neutrons determined the electron abundance, but the new calculations demonstrate that Gamow-Teller electron captures and  $\beta$ -decays involving nuclei are more important [Hix03].

It is therefore important to experimentally constrain theoretical predictions for Gamow-Teller strength over the entire relevant mass range. This is especially true beyond the *pf*-shell, where accurate shell model calculations become difficult and the model-assumptions become questionable. Theoretical methods, for example employing mean-field techniques, are being used [Hix03] that have hardly been tested against experiment. It is crucial that such tests are performed; charge-exchange reactions can provide these necessary data, as is detailed in Section 2.7. Tests of strength distributions in unstable nuclei are especially important, since almost no experimental information is available beyond the small fraction that is accessible by  $\beta$ -decay.

Following the core-collapse process, the neutron star cools by emitting neutrinos, a high flux of neutrinos passes through the overlying shells of heavy elements, and nuclear transmutations via neutrino interactions are induced. Neutral current reactions, induced by energetic  $\mu$  and  $\tau$  neutrinos and their antiparticles are especially important, but charged-current reactions play a role as well. The excitation of the Gamow-Teller resonance state is possible, but due to the high energy of the neutrinos, the excitation of the giant dipole resonances through first-forbidden weak transitions becomes important. This neutrino-process is thought to be largely responsible for the production of a number of rare isotopes, including many of the odd- $Z$  nuclei from boron to copper and nuclei such as  ${}^7\text{Li}$ ,  ${}^{11}\text{B}$ ,  ${}^{19}\text{F}$ ,  ${}^{138}\text{La}$ , and  ${}^{180}\text{Ta}$  [Woo90]. The uncertainties in the calculations, which employed rather simple models for the strength distributions, can be reduced by measurements of the relevant forbidden weak strengths via charge-exchange reactions. In the case of unstable nuclei, these resonances can be probed at the ISF using the (p,n) reaction in inverse kinematics as described in Section 2.7

In addition to weak interactions, a range of other nucleosynthesis processes involving unstable nuclei takes place in core-collapse supernovae. This might possibly include the r- and p-processes, which are discussed separately in Sections 3.2.1 and 3.2.2 respectively. A particularly important process in core-collapse supernovae is the  $\alpha$ -process, which produces the  $\gamma$ -ray emitter  ${}^{44}\text{Ti}$ .  ${}^{44}\text{Ti}$  decay  $\gamma$ -rays have been observed directly from the CasA supernova remnant by  $\gamma$ -ray observatories and  ${}^{44}\text{Ti}$  has also been found incorporated in certain meteorites, where it can be identified through its decay product. The decay of  ${}^{44}\text{Ti}$  also powers the late-time

light-curve of core-collapse supernovae. The amount of  $^{44}\text{Ti}$  produced in a supernova can therefore be inferred from light curve observations, as has been done for supernova 1987a, for example. Such observations pose strong constraints on supernova models, provided the reaction rates relevant for  $^{44}\text{Ti}$  production are accurately known. While some of the important reactions occurring on stable targets or the long-lived  $^{44}\text{Ti}$  itself have been investigated experimentally [Nas06,Son00],

## Core-collapse supernovae

Core-collapse supernovae are the result of the collapse of massive stars (at least eight times the mass of the Sun) that have exhausted the fuel to drive the fusion process and end up with a core that has been converted into iron. The outward thermal pressure from the nuclear reactions no longer balances the massive gravitational force and the star collapses. The density of the material in the star rapidly increases during the implosion and when the density exceeds nuclear matter density, the core rebounds, generating an outgoing shockwave. The shock-wave induces an explosion with an energy release of no less than  $10^{53}$  ergs and nuclear material is disseminated into the interstellar medium leaving behind a variety of remnants that can be observed (Figure A).

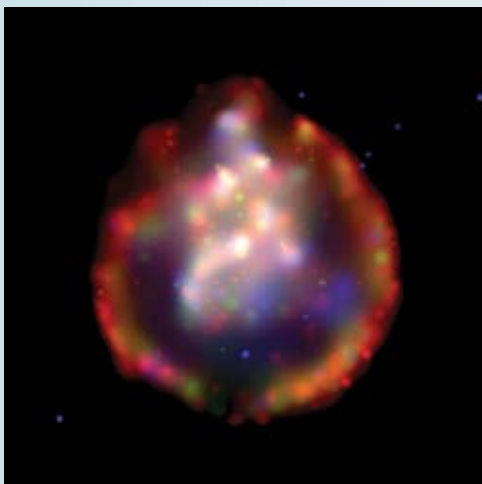


Figure A: Image of the supernova remnant SNR 0103-72.6 in the Small Magellanic Cloud taken by the Chandra X-ray Observatory. The remnant is about 10,000 years old (as seen today) and the ejected material has expanded to a radius of about 75 light years. The colors indicate different X-ray wavelength ranges. Spectral analysis provides information on the chemical composition across the remnant [Par03]. With images such as this, one can directly study supernova nucleosynthesis and the distribution of the elements in the ejecta. Image credit: NASA/CXC/SAO.

A large fraction of nuclei in the universe is thought to stem from core-collapse supernovae and since the supernovae are possible sites for the r-process, a substantial effort is currently going into unraveling the mechanism of the explosion. One of the major puzzles is that present simulations of the collapse are not able to convincingly produce an explosion; the outgoing shock wave stalls before reaching the surface

of the star. Therefore, theoretical efforts are focused on finding new mechanisms that can reenergize the shock wave [Woo05]. Improvements and additions to the current models are necessary, including the description of hydrodynamical properties like convection, asymmetries in the shock-wave process (Figure B), and the transport of radiation (in particular neutrinos) through the star [Fry04,Bur95,Kif06,Mez98,Lie05,Wal05,Bur06].



Figure B: Results of a three-dimensional simulation of the supernova explosion of a 15 solar-mass star [Fry04]. The simulation (here shown 40 ms after the bounce at nuclear density) was designed to study asymmetries in the explosion that may explain observations such as variations in  $\gamma$ -ray spectra, nucleosynthesis yields, and the shape of remnants. Image credit: C.L. Fryer and M.S. Warren.

Another crucial element in the description of supernovae is the accurate treatment of the nuclear reactions, in particular weak transitions among medium-heavy nuclei [Lan03]. The temperatures and densities inside the star are high, so that unstable nuclei that do not normally exist constitute a significant fraction of the matter inside the star. However, the accuracy of the theoretical calculations of weak reaction rates of unstable nuclei is not known, resulting in large uncertainties in the simulations. The calculations of the weak reaction rates must, therefore, be tested and further developed based on experimental data. Such data can be collected by studying charge-exchange reactions in inverse kinematics on unstable nuclei. The ISF will produce suitable beams of unstable nuclei at sufficient intensities to study the whole region of nuclei important for supernovae explosions.

proton capture on the unstable  $^{45}\text{V}$  has also been identified as critical [The98]. With a reaccelerated rare isotope  $^{45}\text{V}$  beam at the ISF, a direct measurement of this reaction rate would be possible (see Section 3.2.3. for a more in-depth discussion of this technique). With such a measurement, the  $^{44}\text{Ti}$  yield of supernova models could be calculated much more reliably.

### 3.2.2.2 Thermonuclear supernovae (type Ia)

Thermonuclear supernovae (type Ia) make half of the iron-group elements in the universe and are crucial standard candles for determining the equation of state of dark energy. Despite their importance, open questions abound. The canonical Type Ia supernova model is a carbon-oxygen white dwarf, accreting matter from a companion star and growing in mass to near the Chandrasekhar limit, where an explosive process ensues. The nature of the binary systems involved is unclear. The extent to which the composition and age of the host stellar population affects the explosion is also uncertain. Multidimensional studies [Gam04,Ple04,Rop06] of the explosion have been performed, but the exact nature of the explosion, whether there is a transition from deflagration to detonation, for example, is still a matter of debate [Thi04].

Weak interactions can again play an important role in the explosion and the accompanying nucleosynthesis. During the explosion, the thermonuclear flame leaves an equilibrium distribution of iron-peak nuclei in its wake. Electron captures on these nuclei lower the pressure of the fluid, which retards the expansion of the star. Electron capture also reduces the amount of radioactive  $^{56}\text{Ni}$  produced and thereby reduces the brightness of the explosion. The amount of  $^{56}\text{Ni}$  produced is also affected by trace neutron-rich isotopes, such as  $^{22}\text{Ne}$ . These are inherited from the progenitor white dwarf [Tim03]. Understanding these effects is necessary for a reliable description of systematic trends in Type Ia supernova brightness [Pod06].

Because these supernovae produce about half of the iron-group nuclei, they must not overproduce these isotopes by more than a factor of two, compared to abundances in the solar system. This constrains the explosion models, the central density of the progenitor white dwarf, and the flame speed [Iwa99]. However, one-dimensional simulations are also sensitive to the weak reaction rates used [Bra00]. If one is confident that the employed rates are reliable, one can use the nucleosynthesis patterns in the iron group to limit the central density and flame speed and, hence, validate evolution models. To have confidence in this procedure, the weak rates used in such models must be tested against experiments. Neutron-rich nuclei in the *pf*-shell are key; the lack of data for unstable nuclei in this region is an important limitation on an accurate description of Type Ia supernovae [Bra00].

### 3.2.2.3 Weak rates for supernovae simulations

In both core-collapse and thermonuclear supernovae (Type Ia), temperatures and densities are so high that energetic electrons can overcome negative electron capture thresholds, and electron captures on unstable neutron-rich nuclei become important. This is also the case for electron captures in neutron star crusts as discussed in Section 3.3.1. The relevant strengths cannot be studied with  $\beta$ -decay experiments under terrestrial conditions. However, charge-exchange reactions can be used to provide the experimental Gamow-Teller strengths necessary [Ost92] to validate theoretical nuclear structure models.

How this is done is shown in Figure 3.6 for the case of electron-capture on the ground state of  $^{58}\text{Ni}$  populating states in  $^{58}\text{Co}$ . Forward angle cross sections for the  $^{58}\text{Ni}(t,^3\text{He})$  reaction [Col06] are proportional to the Gamow-Teller strength for transitions to the same states. In the top left panel of the figure, the measured strength distribution is compared with large-scale shell model calculations [Hag04] using the GXFP1 interaction [Hon04]. The calculation misses the strongest state, near an excitation energy of 2 MeV, but does well at higher energies. In contrast, the calculation using the KB3G interaction [Pov01] describes the data well at low energies

## Thermonuclear supernovae

Thermonuclear (Type Ia) supernovae are thought to be the incineration of a carbon-oxygen white dwarf that accretes mass from a companion star (see Figure A). As the mass of the white dwarf approaches the Chandrasekhar limit (1.4 solar masses), the white dwarf contracts, the temperature in its center increases, and eventually the fusion of carbon nuclei in the interior heats the star faster than it can cool, leading to a runaway thermonuclear reaction that disrupts the white dwarf.



Figure A: Artist's impression of a white dwarf accreting material from a companion red giant in a binary stellar system. As the accreted material pushes the mass of the white dwarf near the Chandrasekhar limit, a runaway thermonuclear reaction launches a flame that incinerates the white dwarf and induces the supernova explosion. Image credit and copyright: David A. Hardy & PPARC.

The subsequent radioactive decay of the fusion products releases approximately  $10^{51}$  ergs of energy and the supernova becomes as bright as its entire host galaxy (see Figure B). Type Ia supernovae are thought to produce about one-half of the iron-group nuclei in the cosmos and have the important added use as standard candles for measuring galactic distances and hence the geometry of the universe. The peak brightness of the explosion is correlated with the rate at which the explosion dims, enabling astronomers to calibrate the distance to faraway supernovae. The deduction that the universe is expanding was made by combining this information with a measurement of the redshift of the emitted light [Rie98,Per99].

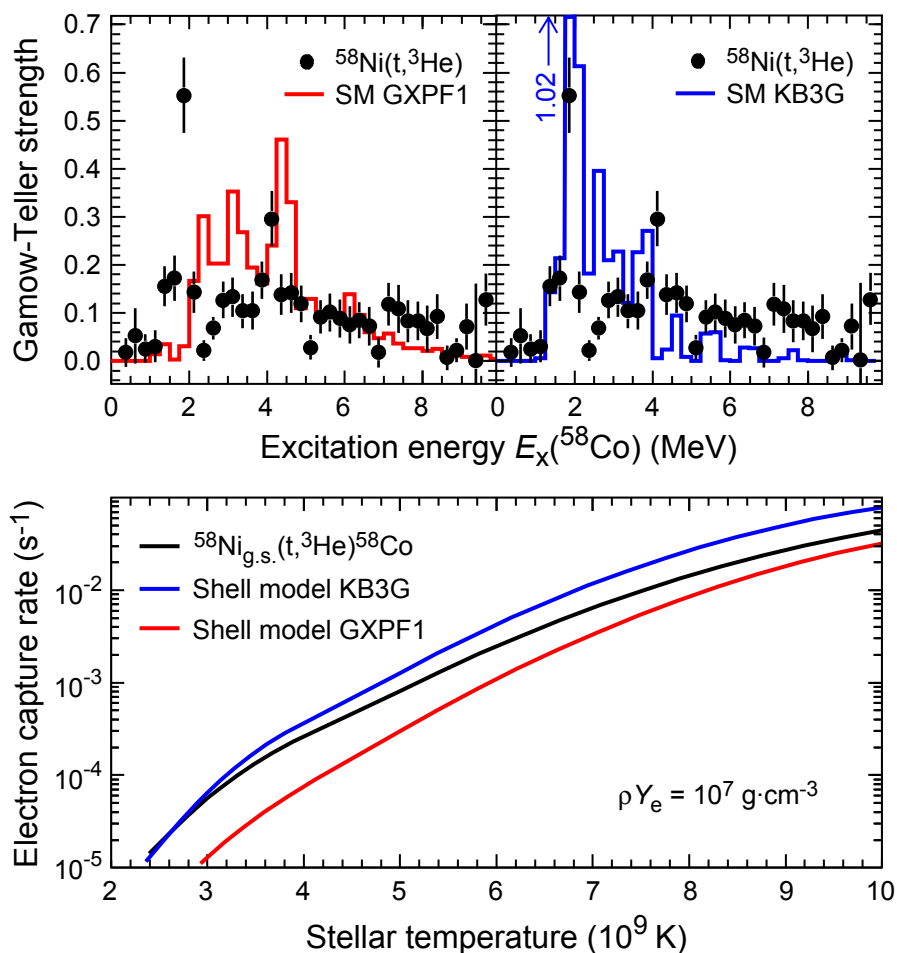


Figure B: Image of the type Ia supernova 1994D observed with the Hubble Space Telescope in the Galaxy NGC 4526 at a distance of 108 million light years. The supernova is located in the lower-left corner and outshines the entire galaxy. Image credit: NASA, ESA, The Hubble Key Project Team, and The High-Z Supernova Search Team.

Despite their cosmological importance, many aspects of Type Ia supernovae are uncertain, including the nature of the progenitor system—is it really an accreting white dwarf? Recent studies suggest that there may be more than one type of progenitor [Man06] and there is the possibility that the calibration of the distance scale of the universe may be affected by changes in the composition of the white dwarf [Pod06]. Since Type Ia supernovae make about 50% of the iron-group nuclei in the universe, the isotopic abundances produced by different explosion scenarios can be tested against the solar abundance pattern. The ISF will play a critical role in allowing studies to constrain the weak reaction rates that are important in Type Ia explosions.

but fails to reproduce the high-energy tail (top right). As a consequence, at low stellar temperatures, the low-energy region of the Gamow-Teller strength distribution is most important for driving electron-captures, and the theoretical calculation employing the KB3G interaction (bottom panel) will be more accurate. This applies, for example, to the precollapse stage of a massive star. At higher temperatures, where weak transitions to high-lying states become increasingly important, the GXPF1 interaction provides more accurate rates. This applies to later stages of the core collapse.

Studies such as these should be performed for a wide range of nuclei and used to improve the shell model interactions and other input for the theoretical calculations. Ideally, this would lead to a consistent and realistic description of weak-transitions rates under a large variety of stellar conditions (e.g., density and temperature) and during the various stages of stellar evolution where different regions on the nuclear chart play a role.



**Figure 3.6:** Comparison of the Gamow-Teller strength distribution in  $^{58}\text{Co}$  extracted from  $^{58}\text{Ni}(t,^3\text{He})$  data at 115 MeV/nucleon [Col06] and large-scale shell model calculations [Hag04], with the GXPF1 interaction [Hon04] (top left) and the KB3G interaction [Pov01] (top right). The bottom panel shows electron-capture rates based on the experimental and theoretical Gamow-Teller strength distributions and for conditions during the precollapse stage of a massive star (density ( $\rho$ ) times electron fraction ( $Y_e$ ) of  $10^7 \text{ g cm}^{-3}$ ). Adapted from [Col06].

---

Experimental data on weak-interaction strengths of relevance for supernovae is restricted, with very few exceptions, to stable nuclei (see Section 2.7). In addition, the bulk of those experiments deal with nuclei in the *pf*-shell, whereas information for heavier nuclei (up to mass  $\sim 120$ ) is equally important. Although some information on electron-capture rates on a few unstable nuclei can be deduced from stable-target experiments by assuming isospin symmetry [Fuj05], it is imperative to extend measurements to the full relevant mass range and to unstable nuclei

As explained in detail in Section 2.7 tools to perform charge-exchange experiments with unstable nuclei in inverse kinematics are currently being developed at the NSCL. Beam intensities required for such experiments must exceed  $10^6 \text{ s}^{-1}$ . As shown in Figure 2.30, the first steps into the unstable neutron-rich region in the relevant mass range (*pf* and *sdg*-shell nuclei) can be made at the CCF, but the ISF will enable one to cover the entire region of interest for type Ia and core-collapse supernovae. Data for a representative set of nuclei, including even-even, odd-odd, and odd-even species and a sampling of the mass range will be necessary and require advanced facilities such as the ISF. This would be sufficient to validate the structure models employed. These models can then be used to produce weak strengths for use in stellar evolution codes that take into account the effects of high stellar temperatures and densities.

Our knowledge of weak-transition rates in stable nuclei could also be rapidly expanded by experiments at the ISF; secondary triton beam intensities would be enhanced by at least two orders of magnitude compared to the capabilities at the CCF, thereby greatly increasing the number of cases that can be studied with the ( $t, {}^3\text{He}$ ) charge-exchange reaction. Such experiments, performed with high resolution and high precision, would enable one to fine-tune the theoretical calculations, further increasing the reliability of the predicted reaction rates.

### 3.2.3 Classical novae

Classical novae are thermonuclear explosions on the surface of a white dwarf, accreting matter from a companion star in a close binary system [Jos05, Geh98, Sta72]. The ashes of the thermonuclear burning are ejected into space and its composition can be observed through spectral analysis. Dozens of novae are observed each year in our Galaxy. After the explosion occurs, the white dwarf continues to accrete matter until the next explosion, with recurrence times being estimated to be typically hundreds of thousands of years. Today several major problems remain unsolved and might indicate severe deficiencies in our understanding of novae. One of the central problems is how and at which stage white dwarf material, either carbon and oxygen, or oxygen and neon is mixed into the accreted surface layer (see [Ale04] for an example of recent work and references therein). These elements can be clearly identified in nova ejecta. This issue might directly determine the ignition condition and is therefore related to the missing mass problem [Sta99] that refers to the fact that many nova models underpredict the total mass of the ejecta compared to observations. Another open question is the contribution of novae to galactic nucleosynthesis. It seems likely that novae are the source of at least a significant fraction of  ${}^{13}\text{C}$ ,  ${}^{15}\text{N}$ , and  ${}^{17}\text{O}$  found in the solar system [Jos05]. They are also possible contributors to the galactic inventory of  ${}^{26}\text{Al}$ , a long-lived  $\gamma$ -ray emitter that has been detected by  $\gamma$ -ray observatories.

Novae are also likely producers of copious amounts of short-lived  $\gamma$ -ray emitters, such as  $^{18}\text{F}$  or  $^{22}\text{Na}$ . So far, existing  $\gamma$ -ray observatories have not succeeded in detecting the corresponding  $\gamma$  rays. An important problem is, therefore, the prediction of production efficiencies for  $\gamma$ -ray emitters in novae in order to judge the necessary sensitivities needed for detection and to interpret any future observations with advanced  $\gamma$ -ray telescopes. This depends directly on nuclear reaction rates. An understanding of the nuclear physics processes during nova explosions is also critical for using observed abundance patterns to constrain nova models and system parameters, such as the white dwarf mass. For example, recent theoretical work, where white dwarf core temperatures and ignition conditions for novae have been calculated self-consistently from the parameters of the binary system, could lead to a solution to the missing mass problem [Tow04]. However, changes in the ignition condition could have dramatic impact on the astrophysical conditions during the explosion and, therefore, on the nucleosynthesis paths. With reliable nuclear reaction rates, one could explore these effects and determine whether the produced abundances of the new models are in agreement with observations. This will either lead to the solution of the problem or reveal further fundamental deficiencies in our understanding of novae.

In summary, the nucleosynthesis in novae depends sensitively on nuclear reaction rates [Cha92,Wie98,Ili02]. Nuclear physics is therefore needed for nova simulations to:

- predict astronomical detection limits for  $\gamma$  rays from radioactive nuclei in matter ejected by novae
- determine the nucleosynthesis contribution of novae, and to novae
- test nova models using the observed composition of the ejecta and to determine the parameters of a particular system

Figure 3.7 indicates the possible reaction flow during a nova explosion. While proton capture rates on stable nuclei are also important, a mild rp-process can develop and proton captures on unstable nuclei can become important. The reactions that have been identified in the past as critical are also marked in Figure 3.7. Because of the sensitivity of the final abundances to these reaction rates, direct measurements with low energy rare isotope beams are needed. Pioneering experiments at existing facilities, such as Louvain-la-Neuve, ORNL, ANL, and ISAC have developed the necessary techniques. Reaction rates with outgoing charged particles have been measured in the past using rare isotope beams (for example [Bar02]), but only very few such reactions play a role in novae. A direct measurement of the proton capture rates requires significantly more beam intensities and have only been possible for very few cases to date [Rui06,Bis03,Dec91]. Some additional rates, especially when stronger resonances are involved, are coming into reach at existing facilities, such as ISAC or the planned development of low-energy beams at the NSCL. These include, for example,  $^{23}\text{Mg}(p,\gamma)$ ,  $^{25}\text{Al}(p,\gamma)$ , and  $^{30}\text{P}(p,\gamma)$  or a few relevant higher lying resonances in  $^{29}\text{P}(p,\gamma)$  and  $^{35}\text{Ar}(p,\gamma)$ . In addition, indirect techniques with rare isotope beams, such as proton scattering (for example [Bar99]), that can be applied with much lower beam intensities have been used. Transfer reaction measurements with stable beams also contributed important information. Though less precise and more model-dependent in their interpretation than the direct measurements, such experiments will continue to improve reaction rate estimates using existing facilities for some cases.

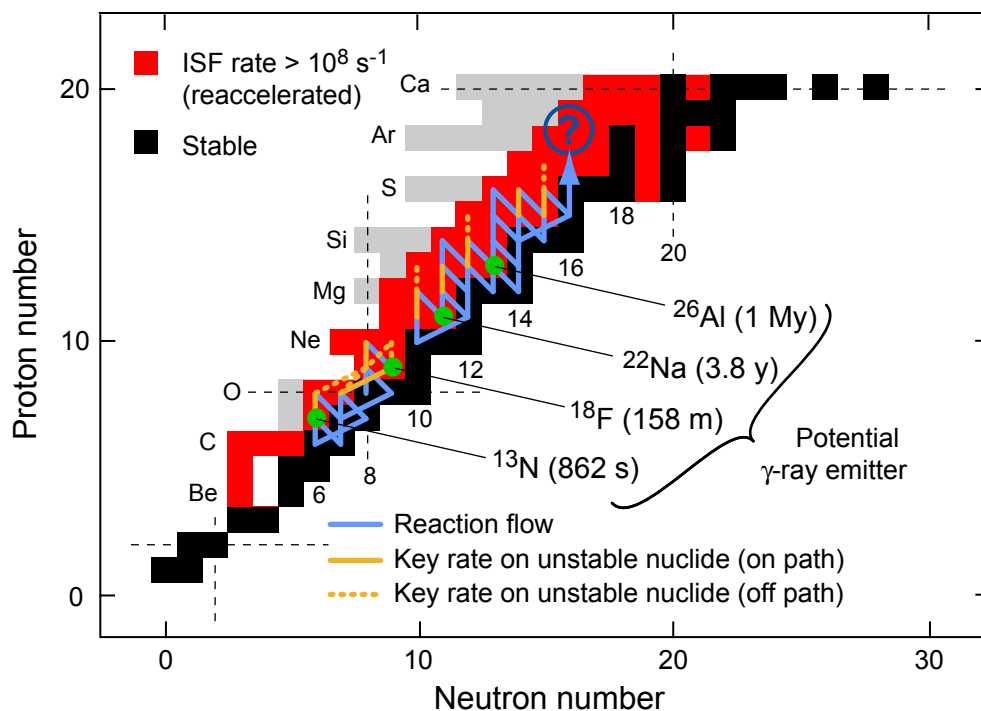


**Figure 3.7:** The reaction flow during a nova explosion on a rather massive O-Ne white dwarf. Dashed lines indicate the classical shell closures. Also shown is the reach of the ISF for reaccelerated low energy rare isotope beam intensities in excess of  $10^8 \text{ s}^{-1}$ . At such beam intensities, many direct reaction rate measurements become possible. Reactions on unstable nuclei that have been identified as important for nova nucleosynthesis in sensitivity studies or other work are marked in orange. Also marked are the nuclei that might serve as potentially observable  $\gamma$ -ray emitters (lifetimes in brackets). An accurate prediction of the abundances of these isotopes is particularly important to guide the search for  $\gamma$ -ray signatures in nova ejecta with  $\gamma$ -ray observatories. Adapted from [Ili99].

The intensities of reaccelerated beams at the ISF will be sufficient for direct measurements of the vast majority of the resonances in all reaction rates relevant for nova nucleosynthesis. Examples include the  $^{27}\text{Si}(p,\gamma)$ ,  $^{29}\text{P}(p,\gamma)$ ,  $^{31}\text{S}(p,\gamma)$ ,  $^{33,34}\text{Cl}(p,\gamma)$ ,  $^{35}\text{Ar}(p,\gamma)$ , and  $^{37,38}\text{K}(p,\gamma)$  reaction rates. With the experimental nuclear astrophysics program at the ISF completed, and with continuing progress at stable beam facilities, the entire nuclear physics of nova explosions will be on a solid basis.

### 3.3 The nature of neutron stars

#### 3.3.1 Crust processes in accreting neutron stars

Matter accreted onto the surface of a neutron star in an X-ray binary system experiences thermonuclear burning via  $\alpha$ -capture reactions, the  $\alpha p$ -process, or the rp-process either in a steady state or explosively in X-ray bursts within hours to days of arriving on the surface (see Section 3.2.1). Even in the most violent X-ray bursts, at most a few percent of the burned matter can be ejected as the gravitational binding energy exceeds the nuclear energy release by at least a factor of 40 [Wei06]. Most of the ashes therefore remain on the surface of the neutron star and are incorporated into the crust by the ongoing accretion. As a fluid element of ashes is continuously compressed, the rising electron Fermi-energy enables a series of

electron capture reactions that drive the composition towards the neutron dripline on timescales of the order of 10–100 years [Han03b]. Once the neutron dripline is reached, the further fate of the matter is not known with certainty and is subject to an ongoing debate. One possibility is that neutron emission and further electron captures produce lighter nuclei that eventually undergo density-induced fusion reactions [Han03b, Gas05, Yak06] (pynuclear fusion reactions are distinct from thermonuclear fusion, which is induced by temperature). Alternatively, neutron captures and  $\beta$ -decays could produce heavier nuclei, driving the crust composition back to its equilibrium composition [Jon05].

Understanding of the nuclear processes in the crust of accreting neutron stars is important because these processes represent the heat sources that set the thermal structure of the crust. They therefore directly affect a number of observables. Prominent examples are superbursts, which are most likely driven by thermonuclear explosions of carbon in a deep liquid ocean located between the solid crust and the gaseous atmosphere where the X-ray bursts occur. The thermal structure of the neutron star crust directly sets the ignition depth and therefore the recurrence time of superbursts [Bro04]. Both can be extracted from observations [Cum06]. It turns out that with our current, very limited understanding of the nuclear physics in neutron star crusts, heating is insufficient to explain the observed superburst properties. This has led some to speculate that superbursts occur on compact stars made of strange matter [Pag05].

Observations of the thermal luminosity emitted by the neutron stars in transient systems during quiescence are another observable of crustal heating. These systems are normal X-ray bursters until accretion shuts off for months or years. Recently it has become possible with X-ray observatories to observe the cooling behavior of the neutron star crust heated by the nuclear processes during the accretion phase [Wij04, Cac06, Sch06a]. Such data could constrain cooling processes and the existence of exotic phases in the neutron star core. A better understanding of the nuclear physics in neutron star crusts is clearly needed to:

- reliably identify the types of nuclear reaction sequences that occur in the crust of an accreting neutron star in model calculations
- determine whether nuclear reactions can heat the crust sufficiently so that deep ignition of carbon is a viable model for superbursts or whether more exotic scenarios are required to explain superbursts
- to interpret superburst and crust cooling observations in terms of neutron star crust and core properties
- to possibly predict additional observational signatures

The critical nuclear physics input are: masses, electron capture rates, and transition schemes for  $A = 20$ – $104$  nuclei ranging from stability to the neutron dripline. These quantities determine the depth at which a particular transition occurs and how much energy is released. Of particular relevance is the location of the low lying electron capture strength in the daughter nuclei to determine the fraction of energy emitted as neutrinos for each transition that is therefore not available to heat the crust. In addition, the strength distribution determines, together with neutron separation energies, to which degree neutron emission can occur before the neutron dripline is reached.

At the ISF, charge-exchange reactions on neutron-rich, unstable nuclei with fast beams can provide information on electron capture strength (see Section 2.7). Further away from stability, measurements of the low lying level structure of neutron-rich nuclei, for example with  $\beta$ -decay spectroscopy, would further constrain electron capture transition schemes predicted by theory. Shell and subshell closures and the associated shape changes are particularly important because they lead to rapid changes in strength distributions over a few isotopes or isotones. This can make crust processes dependent on the initial composition, which determines

## X-ray bursts and neutron star crust processes

Neutron stars accreting matter from a companion star in a close stellar binary system can be observed as bright Galactic X-ray sources. Quasipersistent soft X-ray transients are a subset of these systems [Wij04,Cac06,Sch06a]. They exhibit extended periods of quiescence that can last years, decades, or even longer. Periods of outbursts follow, during which the accretion of matter from the companion star onto the neutron star turns on for years to decades (hence, quasipersistent). During these outbursts, the source brightens by a factor of 100–1000 and, in addition, shows regular X-ray bursts and superbursts.

Nuclear processes thought to occur during the outburst phase include the  $qp$ - and  $rp$ -process in X-ray bursts, explosive carbon burning in superbursts, and the processing of the ashes in the crust by electron captures and pycnonuclear fusion reactions. Pycnonuclear fusion reactions are induced by high density, unlike thermonuclear fusion reactions that are induced by high temperature. These nuclear processes heat the crust and change the temperature profile of the neutron star. Once accretion turns off again, the heating stops and the crust cools down. The current generation of advanced X-ray telescopes such as XMM-Newton and Chandra have observed this cooling behavior.

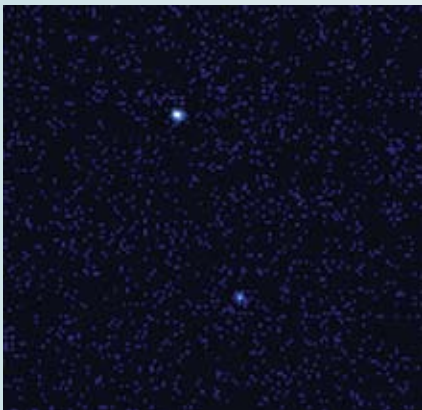


Figure A: Image of the X-ray binary KS 1731-260, observed with the Chandra X-ray observatory about a year after accretion turned off in 2001. Before this time, the object was a bright X-ray source showing normal X-ray bursts and even a superburst. Now the much fainter source is most likely powered by the cooling of the crust that had been heated by nuclear reactions during the accretion phase. Image credit: NASA/CXC/SAO.

An example of this behavior is the object labeled KS 1731-260 (see Figure A) that “turned off” in early 2001 after an active outburst period starting before October 1988. Repeated observations over many years since that time exhibit an exponential cooling behavior (see Figure B) [Cac06]. Both the cooling timescale and the asymptotic behavior can be used to constrain the properties of the crust and the core temperature. This, in turn, provides information about core cooling processes and the possible existence of exotic phases in the center of a neutron star that would alter the cooling processes. Comparison with similar data for another source, MXB 1659-29, revealed differences in the cooling timescale that point to differences in crust properties, possibly due to different composition of the material produced during X-ray bursts. The interpretation of these unprecedented data requires a detailed understanding of the underlying nuclear physics. The relevant nuclear physics includes the properties of the neutron deficient nuclei participating in the  $rp$ -process that occurs during the X-ray bursts observed in the outburst phase. This determines the X-ray burst ashes, which sets the initial composition of the material available for crust heating processes. In addition, the properties of the extremely neutron-rich nuclei participating in the crust heating processes themselves need to be known. Both issues will be addressed by the ISF.

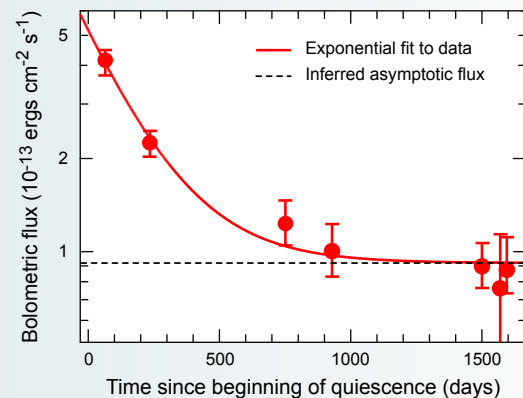


Figure B: X-ray flux from KS 1731-260 after accretion ended, as measured by repeated Chandra and XMM-Newton observations over many years. The drop in flux reflects the cooling of the neutron star crust. This is the first time that the leveling out of the flux to that presumably from the neutron star core has been observed. Adapted from [Cac06].

through which mass regions the electron capture chains ultimately pass until they reach the neutron dripline. Penning-Trap and TOF mass measurements at the ISF would dramatically extend the region of known masses for extremely neutron-rich nuclei (see Section 2.3.1). Finally, experiments with fast beams will also delineate the location of the neutron dripline up to  $A \sim 60$  (see Section 2.1.1) into the relevant mass range for neutron star crust processes. This would be a major step towards a better understanding of neutron star crust processes.

### 3.3.2 The equation of state of dense asymmetric nuclear matter

Macroscopic, strongly interacting dense matter forms the interior of a neutron star and provides the pressure that supports it against gravitational collapse into a black hole. The nuclear symmetry energy provides all of the baryonic contributions to the pressure at saturation density and up to 70% of the pressure at twice saturation density. The symmetric matter EOS provides the remaining hadronic contributions to the pressure. It contributes significantly at densities larger than twice the saturation density but vanishes at saturation density. The EOS in the deep interior governs the maximum mass of neutron stars.

Reflecting its dominant contribution to the pressure, the symmetry energy governs the relationships between the neutron star mass, radius, and moment of inertia. Accurate values for the neutron star masses have been obtained for neutron stars in binary stellar systems, but the radii have not been determined for neutron stars with well-measured masses. Data from NASA's Chandra and the European Space Agency's XMM satellites on omega Cen, M13, 47 Tuc X7, and M28 have provided some information about the radii of neutron stars with unknown masses. Data from EXOSAT, the Rossi X-ray Timing Explorer (RXTE), and XMM have been combined to estimate the radius and mass for the EXO 0748-676 neutron star [Oze06], which is part of a low mass X-ray binary system. Within neutron star models, the radius of  $13.4 \pm 1.8$  km and the high deduced mass  $M = 2.1 \pm 0.3 M_{\odot}$  appear to preclude a soft EOS [Oze06]. These values rely, however, on many possibly incorrect assumptions going into the interpretation of the X-ray spectra. Conclusions would be more quantitative if comparable constraints on the symmetry energy could be provided by laboratory experiments discussed in Section 2.8.1 and by laboratory measurements at even higher incident energies.

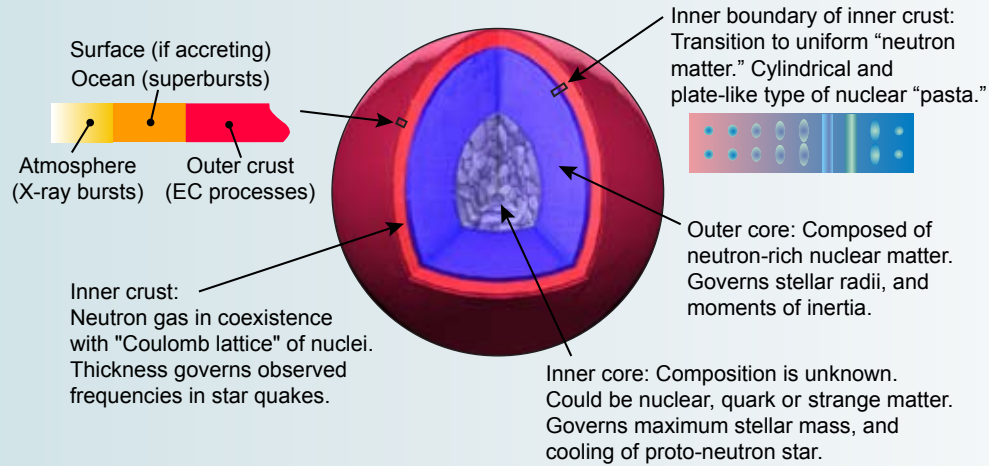
At a given depth in the dense interior, the matter will be in the phase or mixture of phases that has the lowest free energy. The inner crust of the neutron star is expected to be a mixed phase consisting of a Coulomb lattice of denser liquid nuclear droplets embedded in a neutron gas. The thickness of the inner crust, which is sensitive to the density dependence of the symmetry energy at saturation density and below, has recently been constrained by vibration frequencies observed in quakes on the neutron star SGR 1806-20. Experimental constraints on the symmetry energy at this density can be provided by the experiments discussed in Section 2.8.1. Deeper in the core, one may have nuclear matter or strange or quark matter phases depending on whether the symmetry energy of nuclear matter at the relevant density lowers the free energy of nuclear matter below or elevates it above that for the other phases.

The EOS and phase transition in nuclear matter also play a role in the dynamics of core-collapse supernovae. The EOS governs the binding energy of a neutron star formed in the collapse and therefore governs the energy release by neutrinos.

The EOS and the neutrino flux supply the pressure needed for a successful explosion. Neutrino trapping by the in-falling matter depends on the electron capture rates on the nuclei that coexist in a mixed phase along with a gas of nucleons,  $\alpha$  particles, and other light nuclei. The capture rates depend on nuclear masses and isospin asymmetries, which, in turn, depend on the nuclear symmetry energy at subsaturation density and on the relevant nuclear level densities at a range of temperatures. Measurements that could be performed to determine these latter quantities are discussed in Section 2.8.1.

After its birth in a supernova, the neutron star will cool primarily by neutrino emission. The neutrino flux and the cooling rate will be significantly enhanced if the fraction of nucleons that are protons in the stellar core exceeds  $1/9$ , allowing neutrinos to be emitted via the direct nucleonic Urca processes  $n \rightarrow p + e + \nu_e$ ,  $p + e \rightarrow n + \nu_e$  that do not require an additional nucleon collision to conserve momentum. Sufficiently large proton fractions can occur in the inner core if the symmetry energy is strongly density dependent. Measurements that could be performed to constrain the symmetry energy at some of the relevant densities are discussed in Section 2.8.1.

### The structure of a neutron star



The figure shows the complicated layered structure predicted for neutron stars due to the increase in pressure with depth. If a neutron star is part of a binary system, its outer surface may have a thin hydrogen atmosphere and a thin ocean mainly consisting of heavier nuclei produced by thermonuclear burning on the surface. Beneath the ocean of nuclei, the density is such that the neutron star will have a solid outer crust consisting of nuclei embedded in a degenerate electron gas. A transition from the outer crust to an inner crust will occur at the level that electron capture reactions raise the neutron chemical potential to the extent that nuclei can be embedded in a neutron gas. The density of the neutron gas in the inner crust increases with depth and the nuclei, arranged in a Coulomb lattice in this layer, become larger and more neutron-rich with depth. The transition to the outer core of uniform nuclear (mainly neutron) matter may proceed through a variety of geometrical "pasta" phases that start as high as the lower boundary of the inner crust. The nature of the stable phase of the inner core of the neutron star is not known; it could be nuclear matter, quark matter, or consist of pion or kaon condensates. Various astrophysical observables that provide information about these stellar regions are indicated in the figure.